

RESEARCH PAPER



Effect of resveratrol treatment on graft revascularization after islet transplantation in streptozotocin-induced diabetic mice

Eun-Mi Lee^a, Inwon Park^b, Ye-Jee Lee^a, Young-Hye You^a, Ji-Won Kim^a, Myung-Jun Kim^c, Yu-Bae Ahn^a, Pilhan Kim^d, and Seung-Hyun Ko^b

^aDivision of Endocrinology and Metabolism, Department of Internal Medicine, St. Vincent's Hospital, College of Medicine, The Catholic University of Korea, Seoul, Republic of Korea; ^bGraduate School of Medical Science and Engineering, Korea Advanced Institute of Science and Technology, Daejeon, Republic of Korea; ^cDepartment of Physiology, College of Medicine, The Catholic University of Korea, Seoul, Republic of Korea; ^dGraduate School of Nanoscience and Technology, Korea Advanced Institute of Science and Technology, Daejeon, Republic of Korea

ABSTRACT

We evaluated the effect of resveratrol (RSV) on graft survival after islet transplantation (ITx) in diabetic mice. Isolated islets from Balb/c mice (200 IEQ) were transplanted under the kidney capsule of diabetic Balb/c mice. Vehicle or RSV (200 mg/kg/day, orally) was given for 14 days after ITx. Two more control groups [STZ-treated (No-ITx-Control) and STZ+RSV-treated (No-ITx-RSV) mice without ITx] were added. Glucose tolerance tests (GTT) was performed at 14 days after ITx. *In vitro*, isolated islets pretreated with vehicle or RSV (1 μ M) were incubated in a hypoxic chamber (O₂ 1%, 1hr). Some of the ITx was performed in mouse insulin 1 gene promoter-green fluorescent protein (MIP-GFP) transgenic mice and analyzed using an *in vivo* imaging system. After 14 days of ITx, 2-hr glucose levels on GTT in the RSV-treated group were significantly lower than those of other control groups. But the glucose status was not improved in No-ITx mice with RSV. At day 3, the percentage of Ki-67/insulin co-stained cells in islet graft was significantly increased in the RSV-ITx group. Immunostaining with anti-insulin and anti-BS-1 antibodies revealed significantly higher insulin-stained area and vascular density in RSV-treated islet grafts. The mean vessel volume per islet graft measured by *in vivo* imaging was significantly higher in the RSV-treated group at day 3. In isolated islets cultured in hypoxic conditions, the cell death rate and oxidative stress were significantly attenuated with RSV pretreatment. Hypoxic treatment for isolated islets decreased the expression of SIRT-1 mRNA, and this attenuation was recovered by RSV pretreatment. Our data suggest that RSV treatment improved glycemic control, beta-cell proliferation, reduced oxidative stress, and enhanced islet revascularization and the outcome of ITx in diabetic mice.

ARTICLE HISTORY

Received 9 May 2017
Revised 22 November 2017
Accepted 3 December 2017

KEYWORDS

Diabetes; graft survival; *in vivo* imaging; islet transplantation; oxidative stress; resveratrol; revascularization

Introduction

With significant technical improvement and development of knowledge about islet isolation, engraftment, and immunosuppressive treatment, graft survival and the clinical outcomes of islet transplantation (ITx) have been advanced remarkably.^{1,2} The recently published long-term follow-up of the Edmonton Protocol demonstrated that the ITx was associated with long-term islet function, excellent glucose control, avoidance of severe hypoglycemia, and stable renal function without serious infection or malignancy over a period of 11 years.² Therefore, ITx is expected to be one of the possible cure strategies for type 1 diabetes. At the

same time, its application could be extended to limited cases of pancreatitis, or low amount of remnant pancreas after partial pancreatectomy.^{3,4} However, we have to overcome some limitations of ITx, including hypoxic, mechanical, and chemical damage to the transplanted islets.⁵ The success of ITx is dependent on the retrieval of a sufficient amount of fresh islets and maintenance of functioning pancreatic β -cells in transplanted sites. Almost all of the investigations about ITx have been focused on these issues. Therefore, searching for some candidate materials to enhance the function and viability of isolated islets is very important to improve the graft survival after ITx.

CONTACT Pilhan Kim ✉ pilhan.kim@kaist.ac.kr Graduate School of Nanoscience and Technology, Korea Advanced Institute of Science and Technology (KAIST), 291 Daehak-ro, Yuseong, Daejeon, Republic of Korea, 34141; Seung-Hyun Ko ✉ kosh@catholic.ac.kr Division of Endocrinology & Metabolism, Department of Internal Medicine, St. Vincent's Hospital, College of Medicine, The Catholic University of Korea, 93, Jungbu-daero, Paldal-gu, Suwon-si, Gyeonggi-do 442-723, Republic of Korea.

#Eun-Mi Lee and Inwon Park contributed equally to this manuscript.

© 2018 Taylor & Francis

Resveratrol (3,5,4'-trihydroxystilbene, RSV) is a non-flavonoid class of polyphenolic compound, known as a naturally occurring polyphenolic phytoalexin produced by some spermatophytes in response to injury.⁶⁻⁸ RSV is usually found in the skin of red grapes, wine, and berries.⁹ Resveratrol is also reported to activate SIR2 (silent information regulatory 2), an SIRT1 homolog, thus mimicking the benefits of calorie restriction.⁶⁻⁸ It has various metabolic effects in mammalian cells through activation of AMP-activated protein kinase.¹⁰ It also has beneficial effects on glucose homeostasis and insulin secretion.¹¹ SIRT1 functions as a positive regulator of insulin secretion from pancreatic β -cells in response to glucose by directly repressing the uncoupling protein (UCP) gene.¹²

SIRT1 activation has been shown to have anti-inflammatory, anti-apoptosis, anti-cancer, anti-aging, and cardiovascular protective effects in both *in vivo* and *in vitro* studies.¹³ RSV has some beneficial effects on mitochondrial oxidative stress in vascular endothelial cells by activation of SIRT1.¹⁴ SIRT1 is also widely expressed in various endothelial cells, and is known to play a key role in the regulation of endothelial angiogenic functions during blood vessel formation.¹⁵⁻¹⁷ Sufficient revascularization after isolation of islet from donor pancreas is essential to the successful engraftment of transplanted islets. Therefore, if RSV has some beneficial effects on vascular growth, it has also potential benefits for ITx outcomes in the type 1 diabetes model. To investigate the effect of RSV on the revascularization of transplanted islets, we used transgenic mice in which pancreatic β -cells are genetically tagged with green fluorescent protein (MIP-GFP mice) and *in vivo* imaging system.¹⁸

The aim of this study was to investigate the effect of RSV on the survival of transplanted islet grafts in an animal model of type 1 diabetes. We investigated the changes of oxidative stress and revascularization according to RSV treatment after ITx.

Materials and methods

Animal model of type 1 diabetes

Six- to 7-week-old male Balb/c mice (Orientbio, Seongnam, Gyeonggi, Korea) were used as donor and transplant recipients. Mice were housed under standard conditions at $22 \pm 2^\circ\text{C}$ with a 12-h light/dark cycle and standard chow fed ad libitum (Pico 5053, Lab Diet, Brentwood, MO). Type 1 diabetic

model was made using intraperitoneal injection of streptozotocin (STZ: 180 mg/kg, Sigma, St. Louis, MO) dissolved in 10 mM citrate buffer (pH 4.5). If non-fasting glucose levels were maintained above 350 mg/dL for two consecutive days, the mice were used as recipients. All procedures in animal experiments were conducted in strict accordance with approved guideline by the Laboratory Animal Care Committee at the Catholic University of Korea (CUMC-2016-0028-01).

Islet isolation and allogenic transplantation

Islet isolation from mice was performed by ductal infusion of 2 ml of collagenase P (1 mg/ml, Roche, Mannheim, Germany) in M199 medium without fetal bovine serum (FBS; Gibco BRL, Grand Island, NY). After procurement, the pancreas was digested for 25 min at 37°C . Islets were washed and then purified with centrifugation for 25 min at 2,200 rpm using the Histopaque[®]-1077 gradient method (Sigma).^{19,20} Two hundred islet equivalents (IEQs) were collected and transplanted under the left kidney capsule of diabetic mice. On the basis of our experience, we implanted 200 IEQ as a marginal number to temporarily reverse post-transplant hyperglycemia without reaching normoglycemia. After transplantation, blood glucose levels and body weights were monitored every day for 14 days.

RSV treatment and glucose tolerance test (GTT)

The transplanted mice were randomly allocated to two groups: the diabetic control group treated with vehicle (0.5% sodium carboxymethylcellulose, orally once a day, Sigma, $n = 6$, ITx-Control) and the RSV treated group (RSV, 200 mg/kg/day, orally, Sigma, $n = 6$, ITx-RSV). In addition, to investigate whether glucose homeostasis is improved by the resveratrol effect on transplanted islet grafts or if it is an effect on endogenous beta-cells, we added two other control groups; STZ-treated (no graft, $n = 6$, No-ITx-Control) and STZ-treated+RSV (no-graft, $n = 6$, No ITx-RSV). After 14 days of ITx treatment, the transplanted mice received an intraperitoneal GTT (2 g/kg glucose) after 8 hours of fasting, and blood glucose levels were measured at 0, 30, 60, 90 and 120 min using a glucometer (Roche) after glucose loading.

Isolated islets culture and hypoxic treatment

Isolated islets (100 islets) were pre-incubated in Roswell Park Memorial Institute (RPMI) 1640 medium (Sigma) containing 11.1 mM/L glucose and 10% FBS (Hyclone, Logan, UR). To induce hypoxic injury to isolated islets, culture dishes containing islets were placed in a hypoxia chamber (Galaxy 14S, New Brunswick Scientific, Prairie, WI) containing mixed gas of 1% O₂, 5% CO₂ and 94% N₂ at 37°C for 1 hr. Islets were also pretreated with RSV (1 μM) before 2 h of hypoxic incubation.

To measure cell viability, acridine orange (AO, 100 μg/ml, Sigma) and propidium iodide (PI, 500 μg/ml, Sigma) staining were performed in cultured isolated islets. Islets were visualized using a fluorescence microscope (Zeiss, Oberkochen, Germany). The cell death rate was calculated as a relative percentage of the PI staining area to the area of all cells.

Hydrogen peroxide expression in isolated islets

For the measurement of the oxidative stress level, the cultured islets after hypoxic injury were collected and washed twice with phosphate-buffered saline (PBS) and suspended in 1 ml RPMI 1640 medium. The islets were labeled with 10 μM chloromethyl-2', 7'-dichlorofluorescein diacetate (CM-H₂DCFDA, Molecular probes, Carlsbad, CA) for 20 min at 37°C. After PBS washing, the islets were placed in a new dish and visualized using a fluorescence microscope (AX70, Olympus, Japan). After transferring to digitalized image files, the relative fold change of hydrogen peroxide production was calculated by an image analyzer (Image J, National Institutes of Health, Bethesda, MD).

Real-time reverse transcription polymerase chain reaction (RT-PCR) quantification

Total RNA was extracted from mouse islets using TRIzol Reagent (Invitrogen). cDNA was synthesized using 1 μg of total RNA and SuperScript III reverse transcriptase (Invitrogen), according to the manufacturer's instructions. Aliquots (0.1 μg) of cDNA were used as a template in 20 μl reaction mixtures including 1 × SYBR Mastermix (ABI), 10 pM concentrations of the primer pairs, and 0.4 μl of ROX reference dye. The products were detected with the MyiQ Single-Color Real-Time PCR Detection System (Bio-

Table 1. Primer sequences used for real-time polymerase chain reaction.

Primer	Forward sequence (5' → 3')	Reverse sequence (5' → 3')
SIRT1	CAGTGCATGGTTCCTTTC	CACCGAGGAACACTCTGAT
Insulin 1	GCCCTTAGTGACCAGCTATAATCAG	GGGTAGGAAGTGCACCAACAG
β-actin	TTCCAGCCTTCCTTCTTG	TGGCATAGAGGCTTTACGG

Rad). All primer sequences used for PCR are shown in Table 1. The primers were designed to recognize different exons to eliminate possible DNA contamination. The PCR signal was detected using the MiniOpticon™ real-time system (Bio-Rad). The data were analyzed using Supports Opticon Monitor™ software. This software determines the mRNA transcript level using the threshold cycle (C_T) method based on measurements C_T. Finally, the mRNA level of each target gene, which was normalized to β-actin and relative to a calibrator, was calculated with the 2^{-ΔΔC_T} method.

Immunohistochemical staining of islet grafts and pancreatic tissue and morphometric analysis

After GTT, the mice were sacrificed, and islet grafts and pancreatic tissue were retrieved. The extracted kidney containing the islet graft was fixed in 4% formaldehyde, dehydrated in a graded series of ethanol concentrations, and embedded. The paraffin-fixed tissue sections were rehydrated and incubated overnight at 4°C with anti-insulin (1:200, Abcam, Cambridge, MA), anti-glucagon (1:100, Cell Signaling Technology Inc., Danvers, MA), anti-Ki-67 (1:50, Abcam), and anti-8-hydroxy-2'-deoxyguanosine (8-OHdG, 1:100, Abcam) antibodies. After washing with PBS, the sections were incubated with a goat anti-guinea pig rhodamin antibody (1:100, Jackson ImmunoResearch, West Grove, PA) or a horse anti-mouse FITC antibody (1:100, Vector Laboratories, Inc., Burlingame, CA) at room temperature for 2 hrs. To investigate the vascular network in transplanted islet grafts, the lectin *Bandeiraea simplicifolia* agglutinin-1 (BS-1; a specific marker of endothelial cells) staining was performed. The sections were incubated with the BS-1 (1:50, Sigma) in TBS overnight at 4°C. After washing, the sections were incubated with streptavidin-conjugated Texas Red (1:100, Vector Laboratories, Inc.) for 40 min at room temperature. The images were examined using a confocal microscope (LSM510 Meta, Zeiss, Germany) and obtained digitalized pictures

using image analyzer, which were stored as image files. An average of 7.5 sections per graft tissue block was counted systematically from each graft. Immunostaining color was selected for quantification of the relative intensity per islet graft. Using this technique, the relative intensity of insulin, 8-OHdG, or BS-1 immunostaining from sections per islet graft was evaluated for the determination of the mean values.²⁰ The insulin intensity in the transplanted islet was demonstrated as the relative fold change to control group (insulin-stained area/total islet graft area). The insulin/glucagon ratio was expressed as the relative ratio of insulin-stain area to glucagon-stained area in the endogenous pancreas. β -cell mass was calculated by multiplying the relative percentage of β -cells by the total pancreatic weight.

The percentage of BS-1-stained area/total islet graft area (BS-1-stained area/islet graft area X 100) and Ki-67 and insulin co-stained cell number/total cell number (Ki-67, insulin, and DAPI co-stained cell number/total cell number in islet graft X 100) were also measured. The number of 8-OHdG-stained positive nuclei and total nuclei in the whole islet graft were counted on the average number of 76.9 non-overlapping cells per section per islet graft.

In vivo imaging system

To visualize and quantify the angiogenesis in the transplanted islet in the kidney *in vivo*, a custom-built laser-scanning confocal microscopy system for intravital imaging was utilized.^{21,22} As previously described, continuous-wave laser modules at 488 nm (MLD488, Cobolt), 561 nm (Jive, Cobolt), and 640 nm (MLD640, Cobolt) were used as excitation sources for multi-color fluorescence imaging.²³⁻²⁷ An excitation laser beam raster scanning pattern was produced by a laser scanner consisting of a rotating polygonal mirror (MC-5, Lincoln Laser) and a galvanometer-based scanning mirror (6230H, Cambridge Technology), and then transferred to the back aperture of an imaging objective lens. Two objective lenses (PlanApo λ , 20X, NA 0.75, Nikon; LUCPlanFLN, 40X, NA 0.6, Olympus) were used to visualize the transplanted islets in the kidney of the anesthetized mouse on the XYZ translational stage (3DMS, Sutter Instrument). Fluorescence signals from the kidney were epifluorescently detected by the objective lens and delivered to the photomultiplier tubes (PMT; R9110, Hamamatsu,

Japan) through bandpass filters (BPF1; FF02-525/50, BPF2; FF01-600/37, BPF3; FF01-685/40, Semrock, Rochester, NY). The electric signals from the PMT were digitized by a 4-channel frame grabber (Solios, Matrox, Quebec, Canada) and reconstructed to images with a frame size of 512 \times 512 pixels and a frame rate of 30 Hz.

In vivo kidney imaging for transplanted islet grafts

To perform *in vivo* kidney imaging, transgenic mouse insulin I gene promoter-green fluorescence protein (MIP-GFP) expression mice were kindly provided by Dr. H. Kim at Korea Advanced Institute of Science and Technology.¹⁸ Islets (200 IEQ) were isolated from 8 to 12-week-old age of transgenic MIP-GFP mice and then transplanted into the kidney sub-capsule of STZ-induced diabetic C57BL/6 mice (Orientbio) in the same way as described above. Mice were also treated with RSV or vehicle for 3 days after ITx (n = 3 each), and islet grafts were retrieved at day 3 after ITx. Recipient mice were anesthetized by intraperitoneal administration of a mixture of zolazepam and tiletamine (Zoletil, 20 mg/kg), and xylazine (Rompun, 10 mg/kg). After anesthesia, an incision was made on the previously closed wound, and skin, muscle, and peritoneum on the left flank was minimally dissected until kidney exposure. The graft-bearing kidney was exteriorized and a cover glass was carefully attached to the surface of kidney capsule where islets were transplanted under the capsule. At 2 hours before imaging, blood vessels were fluorescently labeled by intravenous injection of anti-CD31 monoclonal antibody (553370, BD Bioscience) conjugated with Alexa Fluor[®] 647 (A-20186, Invitrogen).

Transplanted islets were fluorescently detected by transgenic MIP-GFP expression.¹⁸ Image registration to remove the breathing-induced motion artifact and image averaging to increase the signal-to-noise ratio (SNR) were performed using a custom-written code (MATLAB, Mathworks, Natick, MA). Wide-field imaging was achieved by registering images obtained with a low-magnification objective lens (20X) in a mosaic manner. Seven random spots inside the islet transplantation site were selected to compare islets and nearby angiogenesis. Forty images of the 2 μ m Z-axis interval up to 80 μ m thickness were acquired with a high-magnification objective lens (40X) to investigate islet graft and vessel volume. Each of the vessels and islet graft volumes in random spots was

quantified using the surface rendering module in the image analysis software (IMARIS, Bitplane, Zurich, Switzerland).

Statistical analysis

The experimental results were presented as mean \pm standard error (SE). Statistical analysis was performed using SPSS version 13 (SPSS Inc., Chicago, IL). To compare the mean values of continuous variables between the groups, the independent sample *t*-test or one-way analysis of variance (ANOVA) was used. $P < 0.05$ was considered to be statistically significant.

Results

Blood glucose level after RSV treatment in ITx

After islet transplantation to diabetic mice, the change of body weight was not different between the control and RSV-treated groups until day 6. However, the mean value of body weight in the ITx-RSV group was significantly higher than that of the ITx-control group after day 7 with ITx (Fig 1A). The non-fasting blood

glucose levels were significantly lower in the RSV group after 2 days of ITx, and this decrease was maintained for 14 days. When we removed the graft-bearing kidney at day 14, the glucose level was significantly increased in both groups (Fig 1B). The mean value of glucose levels during oral GTT (Fig 2A) and the area under the curve of glucose (AUCg, Fig 2B) showed that RSV treatment significantly attenuated hyperglycemic status in ITx mice compared to those of the control group. Without ITx, the changes of body weight, non-fasting glucose levels, the mean value of glucose levels during oral GTT, and the area under the curve of glucose (AUCg) were not different between the No-ITx-Control and No-ITx-RSV groups (Fig 1, 2).

Beta cells and vascular density in islet grafts at day 14

We performed immunohistochemical staining in islet grafts after 14 days of ITx. We found that both insulin (green color) and BS-1 expressions (red color) in the transplanted graft were remarkably increased in the RSV group compared to that of control group (Fig 3A). The

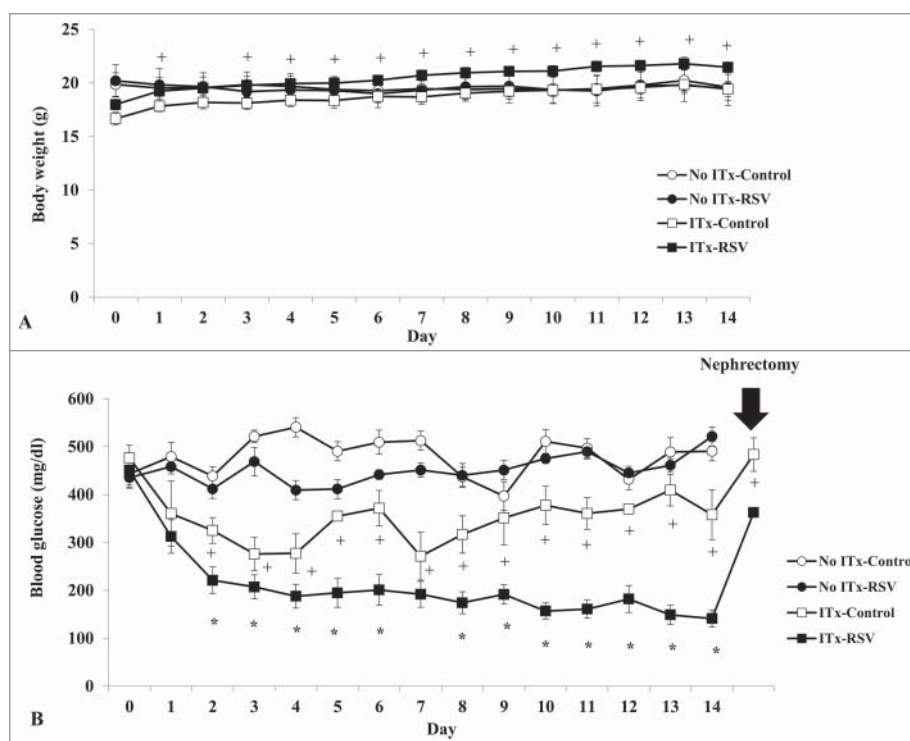


Figure 1. Changes of body weight (A) and non-fasting blood glucose level (B) without and after islet transplantation (ITx) in STZ-induced diabetic mice. (A) Since islet transplantation (ITx), the mean value of body weight was significantly higher in the ITx group (ITx-RSV) than that of the control (ITx-Control) group after day 7 with ITx. + $P < 0.05$, ITx-Control vs. ITx-RSV group. (B) Non-fasting blood glucose level was significantly decreased with ITx-RSV treatment during the observation period of 14 days than those other three groups. Data are expressed as mean \pm SE ($n = 6$ in each group). * $P < 0.05$ vs. other three groups; + $P < 0.05$ vs. ITx-RSV group.

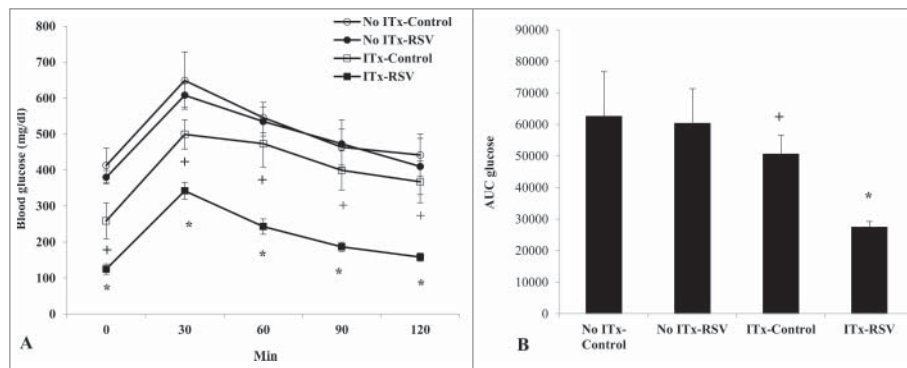


Figure 2. Effects of RSV on glycemic control in diabetic mice without and after ITx. During intraperitoneal GTT, the mean values of blood glucose levels (A) and area under the curve of glucose (AUCg) (B) in the ITx-RSV treatment groups were significantly lower compared to those of control groups. Data are expressed as mean \pm SE ($n = 6$ in each group). * $P < 0.05$ vs. other three groups; + $P < 0.05$ vs. ITx-RSV group.

relative fold increase of the insulin-stained area in the islet grafts of the RSV group was 1.7-fold compared to that of control group ($P < 0.05$, Fig 3B), which correlated with the blood glucose profiles from GTT. When the islet graft was co-stained with BS-1 (endothelial cell marker) and insulin, BS-1 positive cells were scarce in the islet grafts of the control group, while the number of BS-1 positive cells was increased in the RSV group at day 14. The relative percentage of the BS-1-stained area in the graft area was significantly higher in the RSV-treated group than in the control group ($6.1 \pm 2.6\%$ vs. $20.8 \pm 6.1\%$, $P < 0.05$) (Fig 3C).

We also measured endogenous β -cell mass and insulin/glucagon ratio in four experimental groups (Fig 4). We could not find any significant differences in beta-cell mass ($P = 0.482$) and insulin to glucagon ratio ($P = 0.187$) among 4 groups. Regardless of ITx, no effect of RSV on endogenous β -cells was detected.

We also performed immunostaining for Ki-67 both at day 3 and day 14 after ITx. On average, 837.3 cells were counted in graft tissues. At day 3, the percentage of Ki-67-and insulin co-stained cell number/total cell number in graft islet was significantly increased in the RSV-treated group (ITx-Control vs. ITx-RSV group, 1.13 vs 2.47%, $P = 0.036$). But at day 14, the ratio was not different between the two groups (1.09% vs. 0.85%, $P = 0.681$) (Fig 5).

Early revascularization in islet graft using *in vivo* imaging and transgenic MIP-GFP mice at day 3

Early revascularization is important for the engraftment of transplanted islets. We measured angiogenesis at day 3 using *in vivo* imaging and transgenic MIP-GFP mice (Fig 6A). Although there was no difference

in transplanted islet volume between the two groups (MIP-GFP in green color, Fig 6B, C), vascular volume in the islet graft (CD31 in red color, Fig 6B, D) was remarkably increased in the RSV-treated group after ITx. Accordingly, the mean value of the proportion of vascular volume per islet graft was significantly higher in the RSV-treated group (Fig 6E).

Oxidative stress measurement in islet grafts

To investigate the expression of reactive oxidative stress, we performed 8-OHdG and insulin co-staining in islet grafts at 14 days. Compared to the control group, 8-OHdG expression was significantly decreased in the RSV-treated group after ITx (Fig 7). The relative percentage of the number of 8-OHdG-positive cells compared to total cells in islet grafts was significantly lower in the RSV-treated group than that of the control group ($44.3 \pm 12.4\%$ vs. $16.3 \pm 14.5\%$, $P < 0.05$) (Fig 7B).

In vitro hypoxic treatment to isolated islets

When isolated islets were incubated in a hypoxic chamber for 1 h, the cell death rate was significantly increased compared to normoxia incubation (Fig 8A). However, RSV pretreatment remarkably attenuated the cell death rate after hypoxic treatment (control vs. 1 h hypoxia vs. RSV-pretreated hypoxia, 20.4 ± 17.3 vs. 41.7 ± 16.8 vs. $20.7 \pm 12.8\%$, $P < 0.05$) (Fig 8C). Additionally, reactive oxygen species (ROS) production stained with CM-H₂DCFDA also increased after hypoxic treatment, but RSV pretreatment significantly decreased the ROS expression (control vs. 1 h hypoxia vs. RSV-pretreated hypoxia, 1.0 vs. 1.45 vs. 0.43-fold change, $P < 0.05$) (Fig 8D). We also measured mRNAs for SIRT-1 and insulin genes in isolated rat islets after

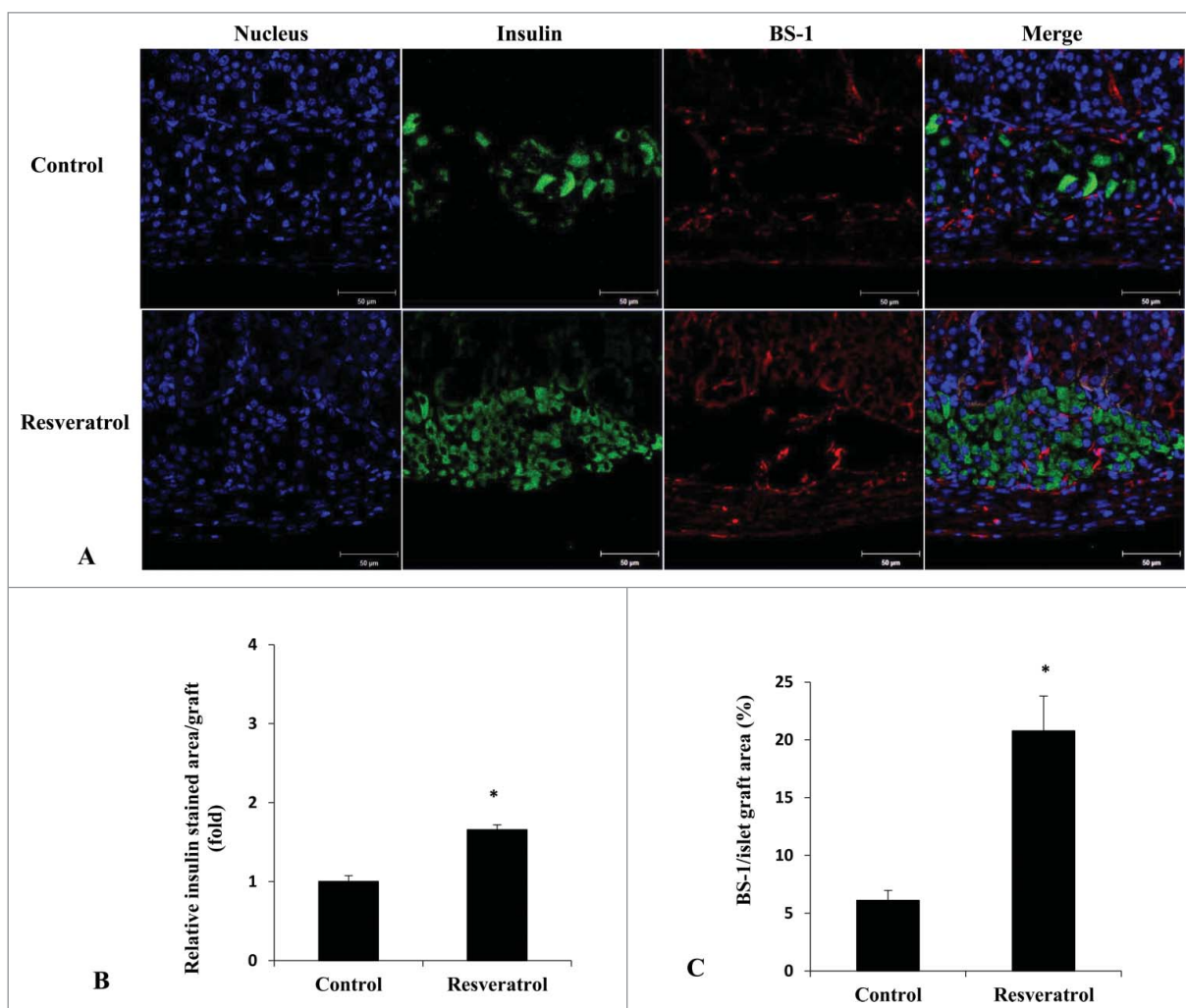


Figure 3. Insulin and BS-1 immunostaining of islet grafts at day 14. (A) RSV-treated islet grafts showed higher insulin (green color) and BS-1 (red color) expression compared with control islet grafts. (B) The relative fold increase of the insulin-stained area in islet grafts of the RSV group was 1.7-fold compared to that of control group. (C) Compared with control group, the relative percentage of the BS-1-stained area in the graft area was significantly higher in the RSV-treated group at day 14. The blue staining is 4',6-diamidino-2-phenylindole (DAPI). Data are expressed as mean \pm SE. * $P < 0.05$ vs. control group.

hypoxic treatment. After hypoxic treatment, both SIRT-1 and insulin mRNA expressions were significantly decreased in the islets compared to the control group. However, RSV pretreatment before hypoxic injury significantly increased the SIRT-1 (Fig 9A) and insulin gene expressions (Fig 9B) compared to hypoxic incubation (Fig 9).

Discussion

In this study, we demonstrated that RSV treatment after ITx improved glycemic control, reduced oxidative stress, and enhanced beta-cell proliferation and islet revascularization in diabetic recipient mice. Although marginal islet mass was transplanted in diabetic mice, which was not enough to

recover diabetes, RSV pretreatment showed significant islet protection effects, which might be related to enhanced early revascularization in graft islets.

Type 1 diabetes is a progressive autoimmune disease characterized by immune-mediated destruction of insulin-producing β -cells within pancreatic islets. Patients should be treated with multiple exogenous insulin injections daily throughout their lifetime. Therefore, ITx is considered an attractive therapy to cure type 1 diabetes. For this reason, the ITx technique has progressed rapidly over the last 40 years, and applied to highly selected patients with type 1 diabetes.^{5,28} However, several obstacles, such as donor availability or selection, engraftment, islet damage during procurement process, and side effects of immunosuppression must

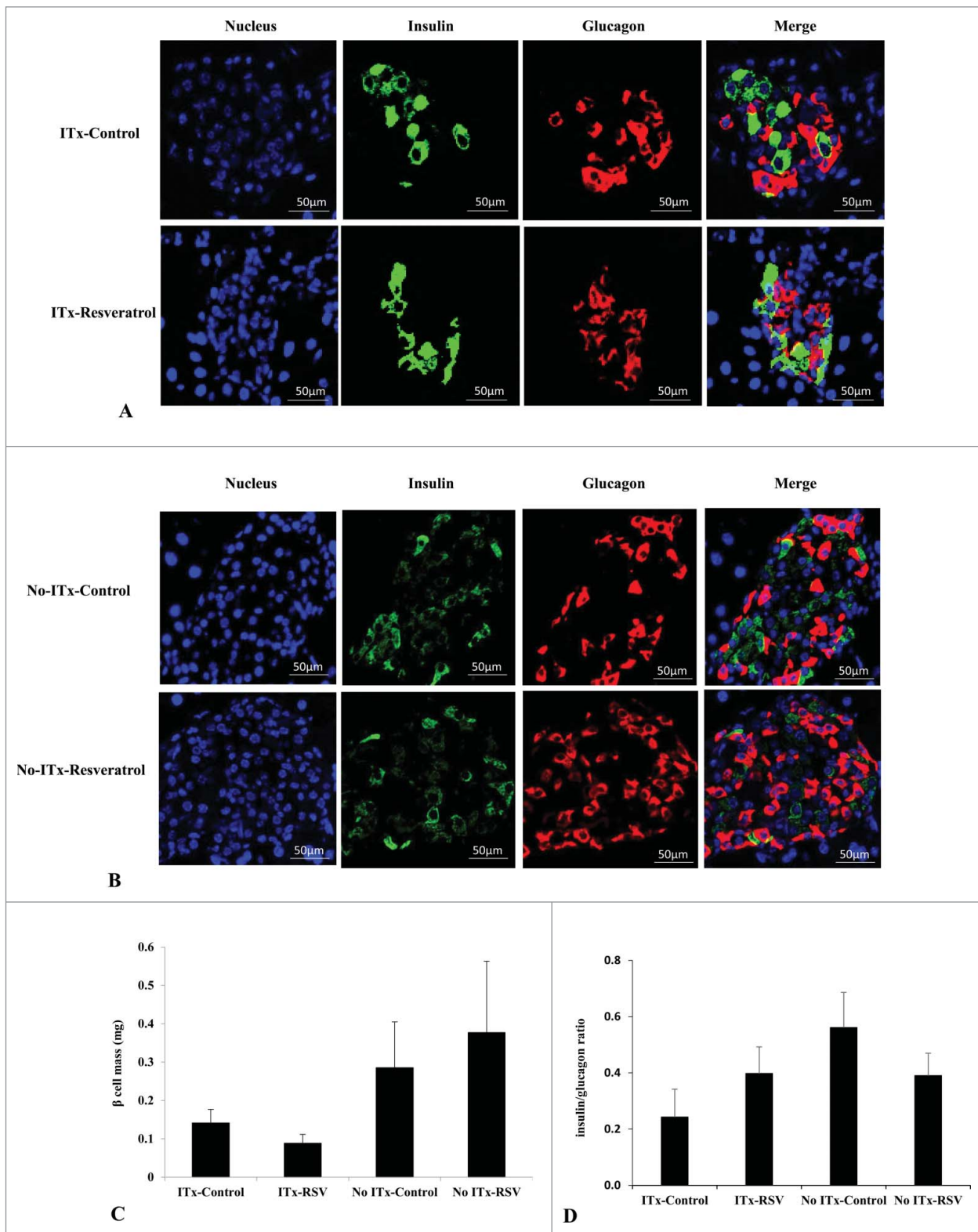


Figure 4. Endogenous β -cell mass and insulin-to-glucagon ratio. Insulin and glucagon immunostaining in the pancreatic tissues of ITx (A) and No-ITx (B) groups. Beta cell mass (C) and the insulin-to-glucagon ratio (D) were not significantly different among the four experimental groups (P value > 0.05 , each). Blue, DAPI-stained cell; Green, insulin-positive cells; Red, glucagon-positive cells. Data are expressed as mean \pm SE ($n = 6$ in each group).

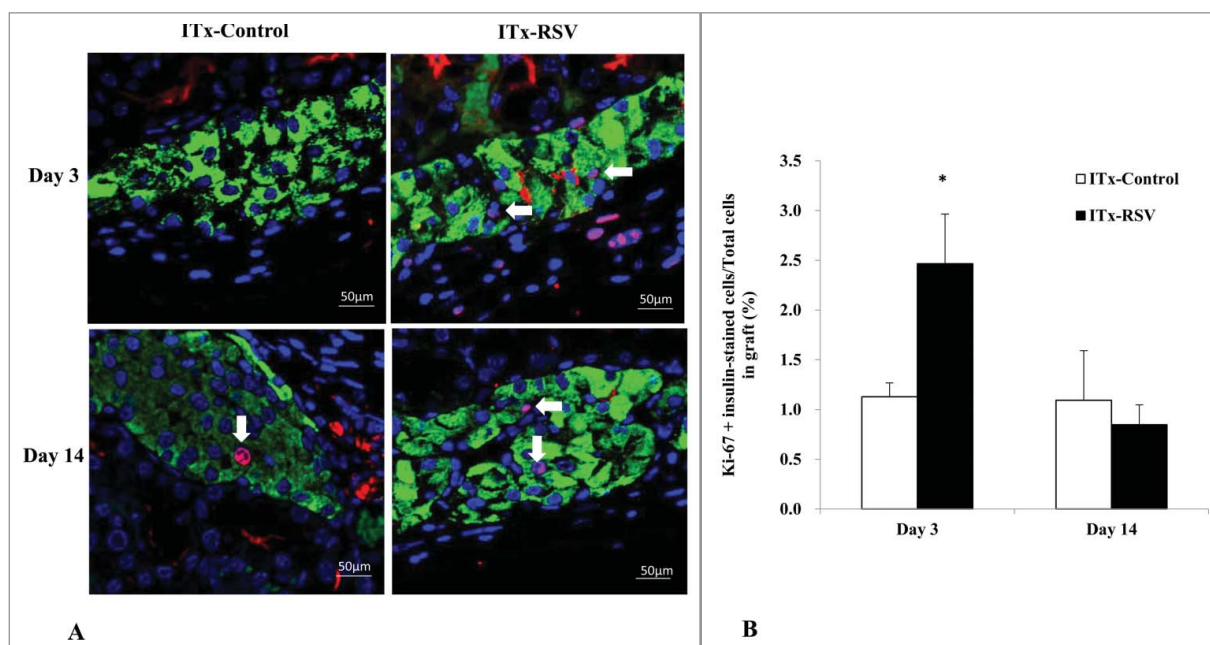


Figure 5. (A) Ki-67 and insulin immunostaining in islet graft tissues at day 3 and day 14 after ITx. (B) At day 3, the percentage of Ki-67 and insulin co-stained cells in islet graft was significantly increased in the RSV-treated group. But at day 14, the ratio was not different between the two groups. Blue, DAPI; Green, insulin; Red, Ki-67 immunostaining. Arrow; Ki-67 and insulin co-stained cell. Data are expressed as mean \pm SE. * $P < 0.05$ vs. control group.

be overcome.^{29,30} Enormous acute stress and injury to islets during this process could be derived from hypoxia, inflammatory cytokines, or oxidative stress.^{15,28} Therefore, a highly pure, viable, and sufficient number of isolated islets with successful revascularization of transplanted islets are critical elements.

SIRT1 is the closest human homolog of the yeast SIR2 protein, known as sirtuin, and regulates longevity and aging in multiple organism models.¹⁵ The major physiologically relevant activity of SIRT1 is the nicotinamide adenine dinucleotide (NAD⁺)-dependent deacetylation of acetylated lysine residues on histone and non-histone substrates.^{6,32} SIRT1 activation is known to have beneficial effects on oxidative stress, inflammation, cellular senescence, apoptosis, metabolism, adipogenesis, circadian rhythms, mitochondrial function, and endothelial dysfunction.³³ Despite the controversy, RSV is still the most potent of the natural SIRT1 activators in vitro, showing enhanced SIRT1-mediated deacetylation by 8-fold.³⁶

Additionally, RSV or SIRT1 activators have proven positive effects on several metabolic disorders, including obesity, insulin resistance, and type 2 diabetes.^{15,35,36} As we have previously published, RSV treatment improved glucose tolerance, attenuated

β -cell loss, and reduced oxidative stress in an animal model of type 2 diabetes.³⁷ From the results that glucose status and endogenous β -cell mass were not improved in No-ITx mice with RSV treatment. We suggested that glucose homeostasis was improved by the resveratrol effect on islet engraftment, vascularization, and β -cell proliferation, rather than its effect on endogenous β -cell protection and/or regeneration.

In addition to the animal model, RSV with natural or synthetic SIRT1-activating compounds, improved glucose homeostasis, showed insulin-sensitizing effects, and decreased oxidative stress and inflammation without adverse side effects in some clinical trials.^{32,38} Despite the beneficial effects of RSV, studies focusing on its therapeutic application to ITx are very limited. Previously, in contrast to the result of our study, McCall et al. demonstrated that RSV (10 and 50 mg/kg/day for 3 weeks after ITx) had no positive impact upon islet engraftment and function or enhancing islet survival in diabetic mice receiving marginal islet grafts.³⁹ We suggest that the discrepancy might be associated with the dose of RSV (200 mg/kg vs. 10–50 mg/kg). We used a relatively high dosage of RSV after ITx. However, in human studies, ingestion of RSV (0.5–3 g/day) was well-tolerated without any

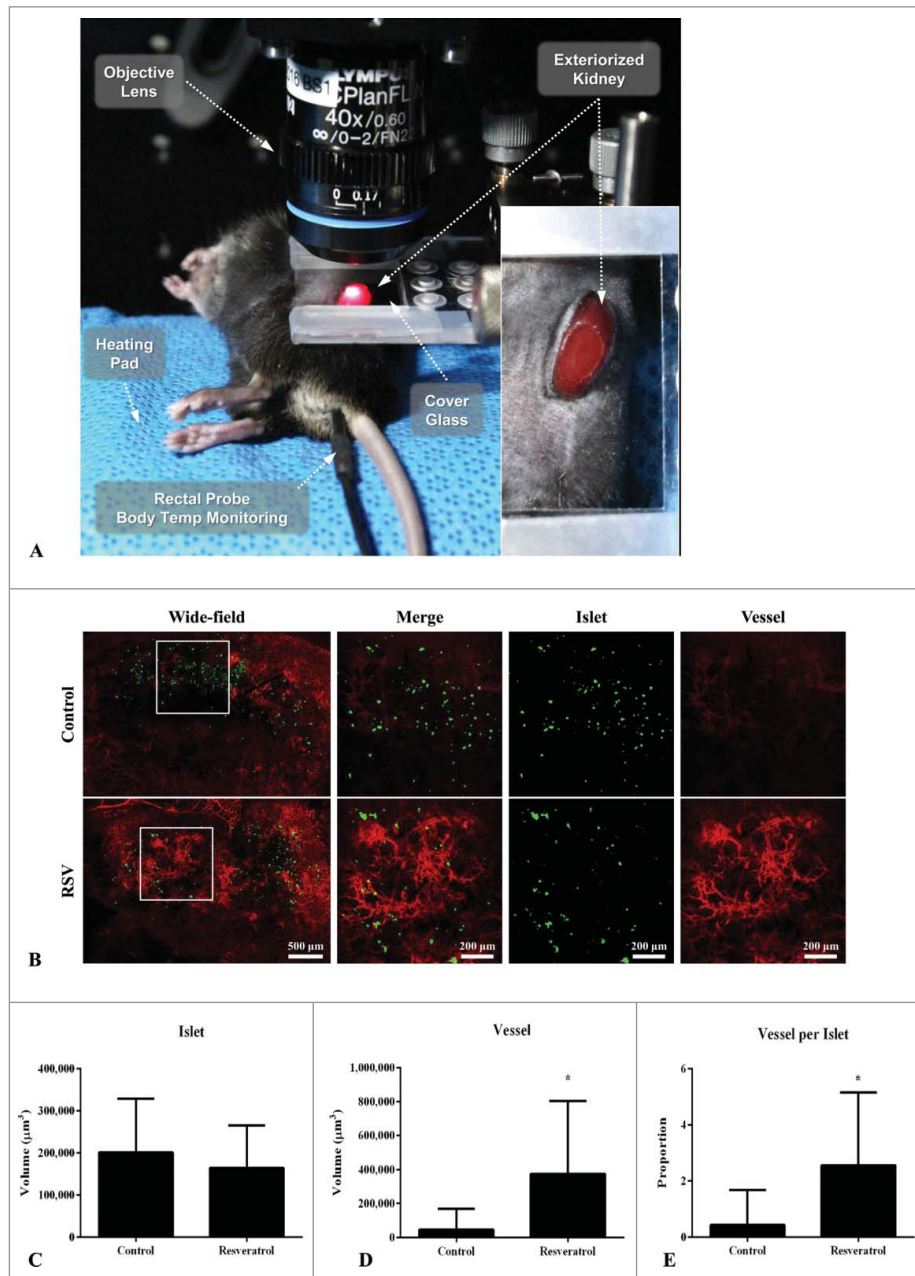


Figure 6. Comparisons of angiogenesis among transplanted kidney islets in the the control and RSV groups at day 3 after ITx. (A) Intravital imaging set up. The laser beam is projected to an animal stage, and *in vivo* imaging can be obtained alive in real time. (B) Representative mosaic intravital images showed merged and vessel images of islet graft in the kidneys in the control and RSV groups (Green: MIP-GFP, Red: CD31). Magnified view of the white box area is depicted in right column representing increased angiogenesis in the RSV group. Graphs of islet volume (C), vessel volume (D), and proportion of vessel volume per islet volume (E) ($n = 20$ fields per group, 3 independent experiments). Data are expressed as mean \pm SD. * $P < 0.0001$.

severe adverse clinical, biochemical, or hematological events.^{30,32,40,41}

Sufficient oxygen and nutrient supply to transplanted islets after ITx should be restored as soon as possible. Angiogenesis following ITx to rebuild their pre-existing capillary network influences the result of ITx.²⁹ This revascularization process initiates within 3 days after ITx and concludes around day

14.^{42,43} Therefore, targeting to enhance angiogenesis is an attractive strategy for successful ITx treatment.

SIRT1 is widely expressed in cultured endothelial cells, the intact aorta of mice, postnatal vascular endothelium, and sprouting endothelial cells, and plays a key role in the regulation of endothelial angiogenic functions during blood vessel formation.¹⁵ RSV treatment also ameliorated endothelial dysfunction by

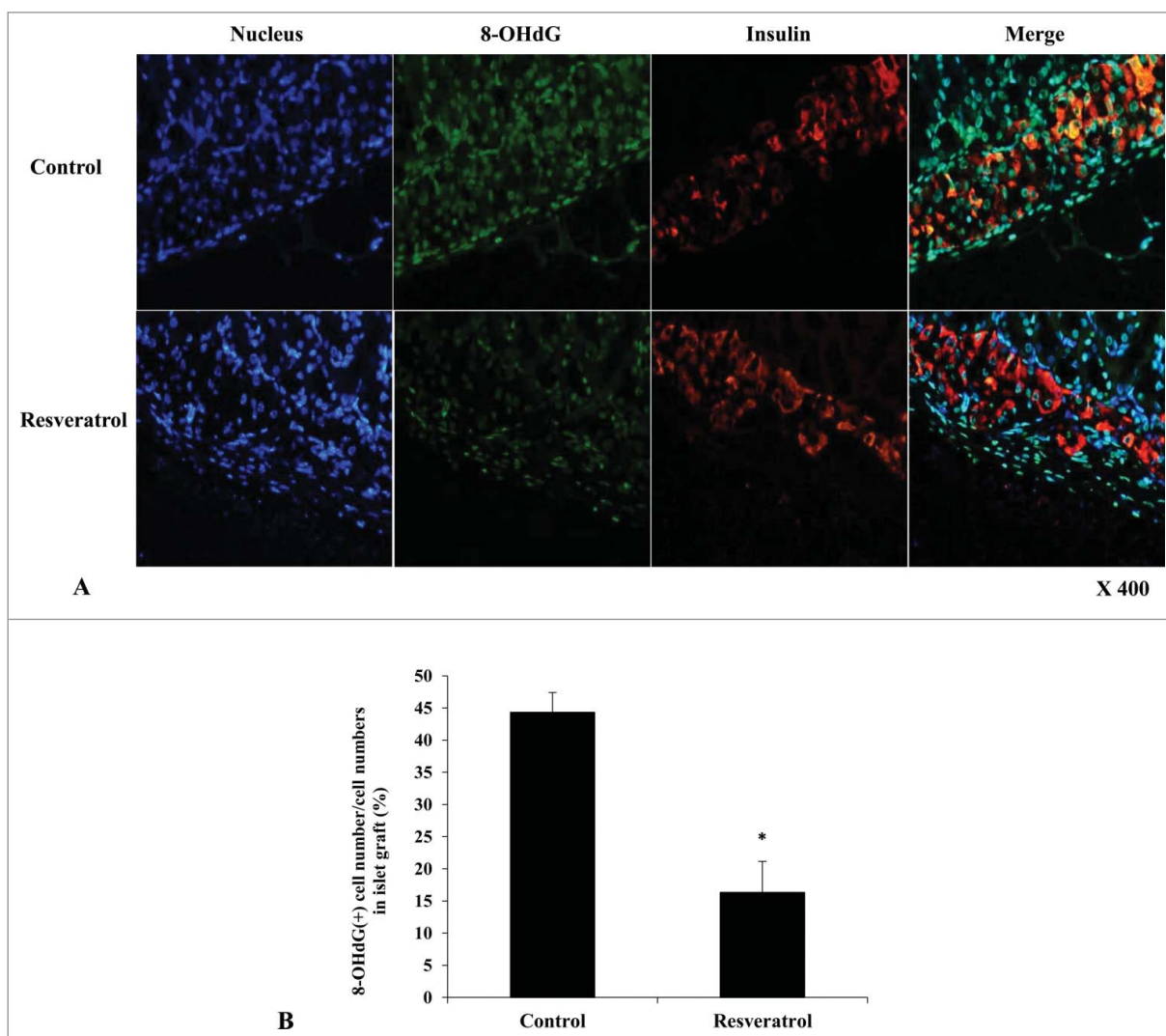


Figure 7. Immunohistochemistry of islet grafts. (A) Compared to control group, 8-OHdG expression (green color) was significantly decreased in the RSV-treated group at 14 days after ITx. DAPI (blue staining) and insulin (red color) were co-stained. (X 400) (B) Relative percentage of number of 8-OHdG-positive cells to total cells in islet grafts was significantly lower in the RSV-treated group compared to that of the control group (* $P < 0.05$).

regulating vascular endothelial growth factor, eNOS, caveolin-1, and heme oxygenase-1 in hypercholesterolemic or ischemic rat myocardium leading to angiogenesis and protection from myocardial injury caused by ischemia-reperfusion.^{9,16,17} To assess neovascularization around the islet grafts after ITx, we used MIP-GFP transgenic mice.¹⁸ Accordingly, BS-1 staining, a marker of microvascular endothelial cells and newly formed blood vessels in the islet engraftment process,⁴⁴ showed that the BS-1-stained area was scarce at day 3 of ITx in control mice; however, it was significantly increased in RSV-treated mice. At day 14, immunohistochemistry with anti-insulin and anti-CD31 antibodies revealed a relatively higher insulin-stained area and greater degree of microvasculature in

the islet grafts, which correlated with significantly improved blood glucose profiles in response to GTT in the RSV-treated group of diabetic recipient mice.

In addition, we found significantly increased Ki-67 and insulin co-stained cells in islet graft at day 3 in ITx-RSV group compared to ITx-control group. We suggest that β -cell proliferation was increased after RSV treatment at day 3 of ITx and contributed to the increase in β -cell-stained area in islet graft at day 14. Therefore, the increased β -cell mass at day 14 of ITx could be explained partially as increased beta-cell proliferation after ITx with RSV treatment at an early stage. We also found that hypoxic treatment for isolated islets decreased the expression of SIRT-1 mRNA, and this attenuation was recovered

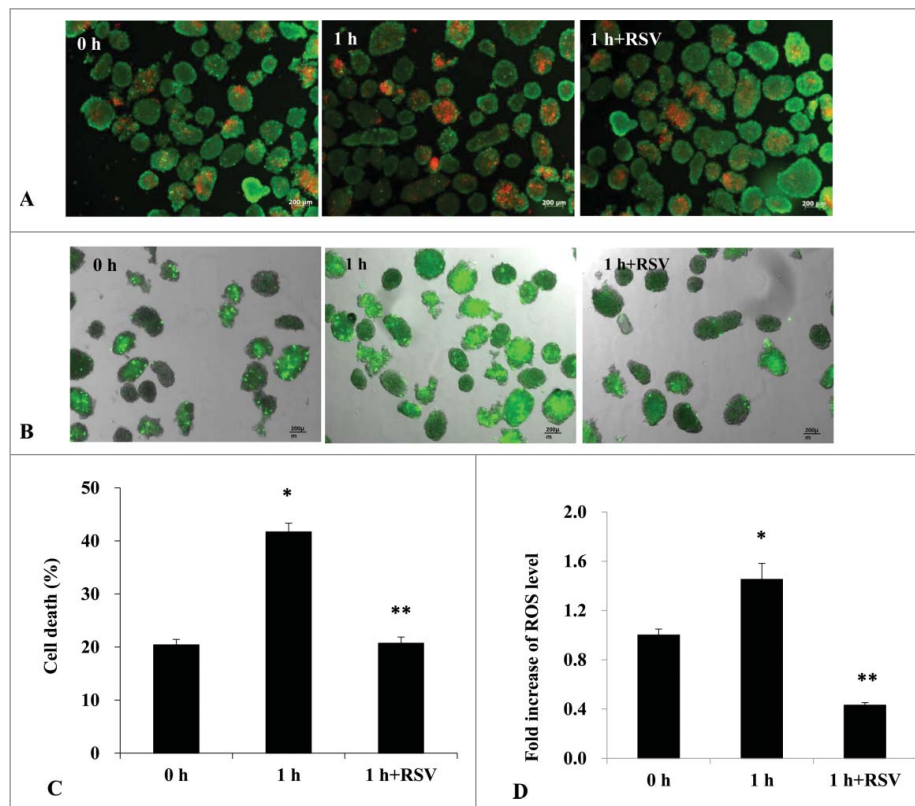


Figure 8. (A) Cell death rate measurement in isolated islets using acridine orange (AO)/propidium iodide (PI) staining (X 50). When isolated islets were incubated in a hypoxic chamber for 1 h, the number of PI-stained cells (red-color) was increased. (B) Hydrogen peroxide staining with CM-H₂DCFDA also increased after hypoxic treatment in isolated islets compared to control islets (X 50). (C) Cell death rate was significantly increased at 1 h of hypoxic conditions compared to normoxia incubation (* $P < 0.05$ vs. control). However, RSV pretreatment remarkably attenuated cell death rate after hypoxic treatment (** $P < 0.05$ vs. 1 h group). Data are expressed as mean \pm SE (n = 3 separate experiments). (D) RSV pretreatment before hypoxic culture significantly attenuated the ROS expression in the islets compared to the non-treated group. Data are expressed as mean \pm SE (n = 3 separate experiments). * $P < 0.05$ vs. control, ** $P < 0.05$ vs. 1 h of hypoxic treatment group.

by RSV, SIRT-1 activator pretreatment. Although we demonstrated the reduction in oxidative stress and improved angiogenesis in the RSV-treated group after ITx, we clearly could not distinguish the

direct effect of RSV on graft islets or the indirect effects of improved revascularization with our findings. But we suggest that RSV accelerated the revascularization process during the immediate

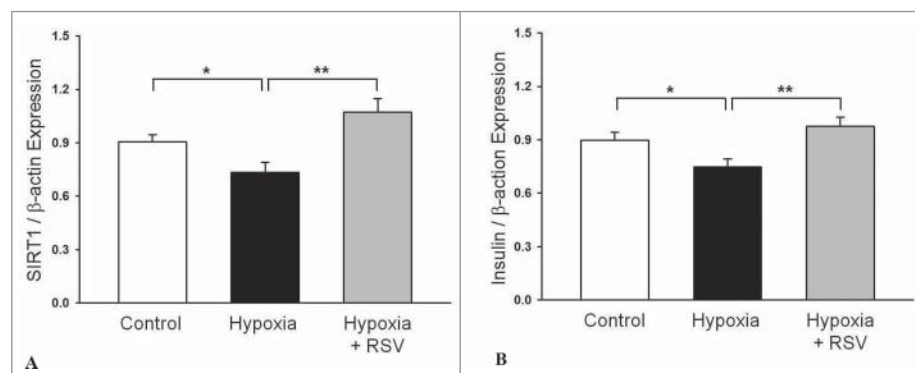


Figure 9. Expression of mRNAs for SIRT-1 (A) and insulin (B) genes in isolated rat islets after hypoxic treatment. After hypoxic treatment, both SIRT-1 and insulin mRNA expressions were significantly decreased in the islets compared to the control group. But RSV pretreatment before hypoxic injury significantly increased the SIRT-1 and insulin gene expressions. Data are expression as mean \pm SE (n = 3 separate experiments). * $P < 0.05$ vs. control, ** $P < 0.05$ vs. 1 h of hypoxic treatment group.

post-transplant period, and contributed to islet graft survival after ITx.

In conclusion, RSV treatment preserved islet mass, attenuated oxidative stress, and enhanced angiogenesis in the early stages of ITx in diabetic mice. RSV treatment could be a promising therapeutic strategy to minimize islet loss in the immediate post-transplantation period and improve ITx outcomes. The pathogenic mechanism of the relationship between SIRT1 activation and angiogenesis should be investigated further in future.

Abbreviations

AO	acridine orange
BS-1	<i>Bandeiraea simplicifolia</i> agglutinin-1
CM-H ₂ DCFDA	chloromethy-2', 7'-dichlorofluorescein diacetate
GTT	glucose tolerance test
IEQ	Islet equivalent
ITx	islet transplantation
MIP-GFP	mouse insulin 1 gene protector-green fluorescent protein
8-OHdG	8-hydroxy-2'-deoxyguanosine
PI	propidium iodide
RSV	resveratrol
STZ	streptozotocin

Disclosure of potential conflicts of interest

No potential conflicts of interest were disclosed.

Funding

This work was supported by Basic Science Research Program through the National Research Foundation of Korea (NRF) funded by the Ministry of Education (NRF-2016R1A2B4008487).

ORCID

Inwon Park  <http://orcid.org/0000-0001-7525-9189>

Seung-Hyun Ko  <http://orcid.org/0000-0003-3703-1479>

References

- Pellegrini S, Cantarelli E, Sordi V, Nano R, Piemonti L. The state of the art of islet transplantation and cell therapy in type 1 diabetes. *Acta Diabetol.* 2016;53(5):683–91. doi:10.1007/s00592-016-0847-z. PMID:26923700.
- Brennan DC, Kopetskie HA, Sayre PH, Alejandro R, Cagliero E, Shapiro AM, Goldstein JS, DesMarais MR, Booher S, Bianchine PJ. Long-Term Follow-Up of the Edmonton Protocol of Islet Transplantation in the United States. *Am J Transplant.* 2016;16:509–17. doi:10.1111/ajt.13458. PMID:26433206. Epub 2015 Oct 3.
- Farney AC, Najarian JS, Nakhleh RE, Lloveras G, Field MJ, Gores PF, Sutherland DE. Autotransplantation of dispersed pancreatic islet tissue combined with total or near-total pancreatectomy for treatment of chronic pancreatitis. *Surgery.* 1991;110:427–37. <https://doi.org/> PMID:1858051.
- Jin SM, Kim KW. Is islet transplantation a realistic approach to curing diabetes? *Korean J Intern Med.* 2017;32:62–6. doi:10.3904/kjim.2016.224. PMID:28049286.
- Shapiro AM. Islet transplantation in type 1 diabetes: ongoing challenges, refined procedures, and long-term outcome. *Rev Diabet Stud.* 2012;9:385–406. doi:10.1900/RDS.2012.9.385. PMID:23804275.
- Baur JA. Biochemical effects of SIRT1 activators. *Biochim Biophys Acta.* 2010;1804:1626–34. doi:10.1016/j.bbapap.2009.10.025. PMID:19897059.
- Frémont L. Biological effects of resveratrol. *Life Sci.* 2000;66:663–73. doi:10.1016/S0024-3205(99)00410-5. PMID:10680575.
- Wenzel E, Somoza V. Metabolism and bioavailability of trans-resveratrol. *Mol Nutr Food Res.* 2005;49:472–81. doi:10.1002/mnfr.200500010. PMID:15779070.
- Baur JA, Sinclair DA. Therapeutic potential of resveratrol: the *in vivo* evidence. *Nat Rev Drug Dis.* 2006;5:493–506. doi:10.1038/nrd2060. PMID:16732220.
- Price NL, Gomes AP, Ling AJ, Duarte FV, Martin-Montalvo A, North BJ, Agarwal B, Ye L, Ramadori G, Teodoro JS, et al. SIRT1 is required for AMPK activation and the beneficial effects of resveratrol on mitochondrial function. *Cell Metab.* 2012;15:675–90. doi:10.1016/j.cmet.2012.04.003. PMID:22560220.
- Moynihan KA, Grimm AA, Plueger MM, Bernal-Mizrachi E, Ford E, Cras-Méneur C, Permutt MA, Imai S. Increased dosage of mammalian Sir2 in pancreatic beta cells enhances glucose-stimulated insulin secretion in mice. *Cell Metab.* 2005;2:105–17. doi:10.1016/j.cmet.2005.07.001. PMID:16098828.
- Bordone L, Motta MC, Picard F, Robinson A, Jhala US, Apfeld J, McDonagh T, Lemieux M, McBurney M, Szilvasi A, et al. Sirt1 regulates insulin secretion by repressing UCP2 in pancreatic beta cells. *PLoS Biol.* 2006;4:e31. doi:10.1371/journal.pbio.0040031. PMID:16366736
- Kitada M, Koya D. SIRT1 in Type 2 Diabetes: Mechanisms and Therapeutic Potential. *Diabetes Metab J.* 2013;37:315–25. doi:10.4093/dmj.2013.37.5.315. PMID:24199159.
- Ungvari Z, Labinskyy N, Mukhopadhyay P, Pinto JT, Bagi Z, Ballabh P, Zhang C, Pacher P, Csiszar A. Resveratrol attenuates mitochondrial oxidative stress in coronary arterial endothelial cells. *Am J Physiol Heart Circ Physiol.* 2009;297:H1876–81. doi:10.1152/ajpheart.00375.2009. PMID:19749157.
- Potente M, Ghaeni L, Baldessari D, Mostoslavsky R, Rossig L, Dequiedt F, Haendeler J, Mione M, Dejana E, Alt FW, et al. SIRT1 controls endothelial angiogenic

- functions during vascular growth. *Genes Dev.* 2007;21:2644–58. doi:10.1101/gad.435107. PMID:17938244.
16. Kaga S, Zhan L, Matsumoto M, Maulik N. Resveratrol enhances neovascularization in the infarcted rat myocardium through the induction of thioredoxin-1, heme oxygenase-1 and vascular endothelial growth factor. *J Mol Cell Cardiol.* 2005;39:813–22. doi:10.1016/j.yjmcc.2005.08.003. PMID:16198371.
 17. Penumathsa SV, Koneru S, Samuel SM, Maulik G, Bagchi D, Yet SF, Menon VP, Maulik N. Strategic targets to induce neovascularization by resveratrol in hypercholesterolemic rat myocardium: role of caveolin-1, endothelial nitric oxide synthase, hemeoxygenase-1, and vascular endothelial growth factor. *Free Radic Biol Med.* 2008;45:1027–34. doi:10.1016/j.freeradbiomed.2008.07.012. PMID:18694817.
 18. Hara M, Wang X, Kawamura T, Bindokas VP, Dizon RF, Alcoser SY, Magnuson MA, Bell GI. Transgenic mice with green fluorescent protein-labeled pancreatic beta β -cells. *Am J Physiol Endocrinol Metab.* 2003;284:E177–83. doi:10.1152/ajpendo.00321.2002. PMID:12388130.
 19. Gotoh M, Maki T, Kiyozumi T, Satomi S, Monaco AP. An improved method for isolation of mouse pancreatic islets. *Transplantation.* 1985;40:437–38. doi:10.1097/00007890-198510000-00018. PMID:2996187.
 20. Zhang N, Richter A, Suriawinata J, Harbaran S, Altomonte J, Cong L, Zhang H, Song K, Meseck M, Bromberg J, et al. Elevated vascular endothelial growth factor production in islets improves islet graft vascularization. *Diabetes.* 2004;53:963–70. doi:10.2337/diabetes.53.4.963. PMID:15047611.
 21. Kim P, Chung E, Yamashita H, Hung KE, Mizoguchi A, Kucherlapati R, Fukumura D, Jain RK, Yun SH. In vivo wide-area cellular imaging by side-view endomicroscopy. *Nat Methods.* 2010;7:303–5. doi:10.1038/nmeth.1440. PMID:20228814.
 22. Han S, Lee SJ, Kim KE, Lee HS, Oh N, Park I, Ko E, Oh SJ, Lee YS, Kim D, et al. Amelioration of sepsis by TIE2 activation-induced vascular protection. *Sci Transl Med.* 2016;8:335ra55. doi:10.1126/scitranslmed.aad9260. PMID:27099174.
 23. Choe K, Hwang Y, Seo H, Kim P. In vivo high spatiotemporal resolution visualization of circulating T lymphocytes in high endothelial venules of lymph nodes. *J Biomed Opt.* 2013;18:036005. doi:10.1117/1.JBO.18.3.036005. PMID:23462969.
 24. Choe K, Jang JY, Park I, Kim Y, Ahn S, Park DY, Hong YK, Alitalo K, Koh GY, Kim P. Intravital imaging of intestinal lacteals unveils lipid drainage through contractility. *J Clin Invest.* 2015;125:4042–52. doi:10.1172/JCI76509. PMID:26436648
 25. Hwang Y, Ahn J, Mun J, Bae S, Jeong YU, Vinokurov NA, Kim P. In vivo analysis of THz wave irradiation induced acute inflammatory response in skin by laser-scanning confocal microscopy. *Opt Express.* 2014;22:11465–75. doi:10.1364/OE.22.011465. PMID:24921268.
 26. Seo H, Hwang Y, Choe K, Kim P. In vivo quantitation of injected circulating tumor cells from great saphenous vein based on video-rate confocal microscopy. *Biomed Opt Express.* 2015;6:2158–67. doi:10.1364/BOE.6.002158. PMID:26114035.
 27. Ahn J, Choe K, Wang T, Hwang Y, Song E, Kim KH, Kim P. In vivo longitudinal cellular imaging of small intestine by side-view endomicroscopy. *Biomed Opt Express.* 2015;6:3963–72. doi:10.1364/BOE.6.003963. PMID:26504646
 28. Korsgren O, Nilsson B, Berne C, Felldin M, Foss A, Kallen R, Lundgren T, Salmela K, Tibell A, Tufveson G. Current status of clinical islet transplantation. *Transplantation.* 2005;79:1289–93. doi:10.1097/01.TP.0000157273.60147.7C. PMID:15912090.
 29. Bruni A, Gala-Lopez B, Pepper AR, Abualhassan NS, Shapiro AJ. Islet cell transplantation for the treatment of type 1 diabetes: recent advances and future challenges. *Diabetes Metab Syndr Obes.* 2014;7:211–23. doi:10.2147/DMSO.S50789. PMID:25018643.
 30. Szkudelski T, Szkudelska K. Resveratrol and diabetes: from animal to human studies. *Biochim Biophys Acta.* 2015;1852:1145–54. doi:10.1016/j.bbadis.2014.10.013. PMID:25445538.
 31. Kanak MA, Takita M, Kunnathodi F, Lawrence MC, Levy MF, Naziruddin B. Inflammatory response in islet transplantation. *Int J Endocrinol.* 2014;2014:451035. doi:10.1155/2014/451035. PMID:24883060.
 32. Knutson MD, Leeuwenburgh C. Resveratrol and novel potent activators of SIRT1: effects on aging and age-related diseases. *Nutr Rev.* 2008;66:591–6. doi:10.1111/j.1753-4887.2008.00109.x. PMID:18826454.
 33. Chung S, Yao H, Caito S, Hwang JW, Arunachalam G, Rahman I. Regulation of SIRT1 in cellular functions: role of polyphenols. *Arch Biochem Biophys.* 2010;501:79–90. doi:10.1016/j.abb.2010.05.003. PMID:20450879.
 34. Hubbard BP, Sinclair DA. Small molecule SIRT1 activators for the treatment of aging and age-related diseases. *Trends Pharmacol Sci.* 2014;35:146–54. doi:10.1016/j.tips.2013.12.004. PMID:24439680.
 35. Lagouge M, Argmann C, Gerhart-Hines Z, Meziane H, Lerin C, Daussin F, Messadeq N, Milne J, Lambert P, Elliott P, et al. Resveratrol improves mitochondrial function and protects against metabolic disease by activating SIRT1 and PGC-1 α . *Cell.* 2006;127:1109–22. doi:10.1016/j.cell.2006.11.013. PMID:17112576.
 36. Baur JA, Pearson KJ, Price NL, Jamieson HA, Lerin C, Kalra A, Prabhu VV, Allard JS, Lopez-Lluch G, Lewis K, et al. Resveratrol improves health and survival of mice on a high-calorie diet. *Nature.* 2006;444(7117):337–42. doi:10.1038/nature05354. PMID:17086191.
 37. Lee YE, Kim JW, Lee EM, Ahn YB, Song KH, Yoon KH, Kim HW, Park CW, Li G, Liu Z, et al. Chronic resveratrol treatment protects pancreatic islets against oxidative stress in db/db mice. *PLoS One.* 2012;7:e50412. doi:10.1371/journal.pone.0050412. PMID:23226280.
 38. Smoliga JM, Baur JA, Hausenblas HA. Resveratrol and health—a comprehensive review of human clinical trials. *Mol Nutr Food Res.* 2011;55:1129–41. doi:10.1002/mnfr.201100143. PMID:21688389.

39. McCall MD, Pawlick R, Shapiro AM. Resveratrol fails to improve marginal mass engraftment of transplanted islets of Langerhans in mice. *Islets*. 2011;3:241–5. doi:10.4161/isl.3.5.16698. PMID:21904116.
40. Boockock DJ, Faust GE, Patel KR, Schinas AM, Brown VA, Ducharme MP, Booth TD, Crowell JA, Perloff M, Gescher AJ, et al. Phase I dose escalation pharmacokinetic study in healthy volunteers of resveratrol, a potential cancer chemopreventive agent. *Cancer Epidemiol Biomarkers Prev*. 2007;16:1246–52. doi:10.1158/1055-9965.EPI-07-0022. PMID:17548692.
41. Vang O. What is new for resveratrol? Is a new set of recommendations necessary? *Ann N Y Acad Sci*. 2013;1290:1–11. doi:10.1111/nyas.12173. PMID:23855460.
42. Emamaullee JA, Shapiro AM. Factors influencing the loss of beta-cell mass in islet transplantation. *Cell Transplant*. 2007;16:1–8. doi:10.3727/000000007783464461. PMID:17436849.
43. Menger MD, Yamauchi J-I, Vollmar B: Revascularization and microcirculation of freshly grafted islets of Langerhans. *World J Surg*. 2001;25:509–15. doi:10.1007/s002680020345. PMID:11344405.
44. Lau J, Kampf C, Mattsson G, Nyqvist D, Köhler M, Berggren PO, Carlsson PO. Beneficial role of pancreatic microenvironment for angiogenesis in transplanted pancreatic islets. *Cell Transplant*. 2009;18:23–30. doi:10.3727/096368909788237131. PMID:19476206.